

# 磁场作用下轴向运动功能梯度 Timoshenko 梁的 振动特性

陈 喜, 唐有绮, 柳 爽

(上海应用技术大学机械工程学院, 上海 201418)

**摘要:** 轴向运动结构的工程振动问题一直是动力学领域中的重要课题之一。为了更全面地分析工程中的振动, 针对磁场作用下轴向运动功能梯度 Timoshenko 梁的振动特性展开论述。基于梁的动力学方程组和相应的简支边界条件, 应用复模态方法, 得到不同参数时固有频率和衰减系数与轴向运动速度的对应关系。采用微分求积法分析磁场作用下前四阶固有频率和衰减系数随轴向运动速度的变化, 并与复模态方法的结果进行对比验证。数据结果表明复模态方法得到的结果是精确解析解。衰减系数呈现不对称性, 耦合固有频率呈现分离性。随着轴速、磁场强度和功能梯度指数的增大, 梁的固有频率减小; 随着支撑刚度参数的增大, 梁的固有频率增大。

**关键词:** Timoshenko 梁; 功能梯度材料; 复模态方法; 固有频率; 衰减系数

**中图分类号:** O326 **文献标志码:** A **文章编号:** 1004-4523(2021)06-1161-08

**DOI:** 10.16385/j.cnki.issn.1004-4523.2021.06.007

## 引 言

随着科学技术的迅速发展, 轴向运动功能梯度结构的磁力控制在航空航天、机械工程和交通运输等领域得到广泛的应用。工程实际中, 机械设备可能处于高温差的环境中或系统受到外部机械力作用而产生较大的振动, 从而降低设备的可靠性和安全性, 甚至带来重大的经济损失。因此, 研究磁场作用下轴向运动功能梯度结构的振动特性具有理论意义和实际意义。

轴向运动结构的研究最早可以追溯到 Aiken<sup>[1]</sup> 的实验观测和分析。许多优秀的综述反映了该领域不同时期的研究进展<sup>[2-8]</sup>。王乐等<sup>[9]</sup>求解自由边界下轴力对 Timoshenko 梁的横向振动影响。Tang 等<sup>[10]</sup>研究了不同边界条件下轴向运动 Timoshenko 梁的固有频率、模态以及临界速度。杨晓东等<sup>[11]</sup>研究了两端铰支边界条件下 Timoshenko 模型轴向运动梁的横向振动问题。刘星光等<sup>[12]</sup>对三种典型轴向运动结构的振动特性进行了对比。Ghayesh 等<sup>[13]</sup>研究了轴向运动 Timoshenko 梁参数振动中的周期响应问题。Chen 等<sup>[14]</sup>研究了黏弹性轴向运动 Timoshenko 梁在参数共振下的动态响应问题。Ghayesh 等<sup>[15]</sup>研究了轴向运动 Timoshenko 梁的非线性受迫振动及其稳定性。周远等<sup>[16]</sup>研究了黏弹性阻尼作用下轴向

运动 Timoshenko 梁的振动特性。唐有绮<sup>[17]</sup>研究了轴向运动黏弹性 Timoshenko 梁的稳态响应。An 等<sup>[18]</sup>通过广义积分变换方法, 研究了轴向运动 Timoshenko 梁的动态响应。文献[19-20]研究了以轴向速度为周期性改变参数的轴向运动 Timoshenko 梁参数振动问题。Hu 等<sup>[21]</sup>建立了磁场环境下轴向运动的导电材料梁的力学模型, 推导了磁弹性振动方程。张立保等<sup>[22]</sup>研究了磁场中轴向运动导电梁的自由振动。文献[23-24]对超导和铁磁材料等构件在电磁场作用下的弯曲、失稳等问题进行了深入的研究。王杰等<sup>[25]</sup>研究了磁场中轴向运动导电梁的主共振问题。胡宇达等<sup>[26]</sup>研究了在平行导线间轴向运动铁磁梁的主共振问题。Liu 等<sup>[27]</sup>研究了磁场中轴向运动导电梁非线性自由振动的位移响应。崔雪<sup>[28]</sup>推导了梁双向振动固有频率和阻尼比的表达式。Su 等<sup>[29]</sup>通过发展动态刚度法, 研究了功能梯度 Timoshenko 梁的自由振动。Zhong 等<sup>[30]</sup>研究了悬臂功能梯度梁在不同载荷作用下的问题。Alshorbagy 等<sup>[31]</sup>基于幂律理论, 研究了材料沿轴向或横向分层的功能梯度梁的动力特性。Lai 等<sup>[32]</sup>导出了功能梯度梁大振幅振动的精确解析解。Thai 等<sup>[33]</sup>发展了功能梯度梁弯曲和自由振动的各种高阶剪切变形梁理论。刘金建等<sup>[34]</sup>研究了幂律指数和剪切变形对功能梯度梁弯曲和自由振动响应的影响, 分析了轴向运动功能梯度黏弹性梁横向振动的稳定性问题。赵

**收稿日期:** 2020-12-03; **修订日期:** 2021-02-06

**基金项目:** 国家自然科学基金资助项目(11672186, 11602146); 上海市自然科学基金资助项目(21ZR1462500, 18ZR1438200)

凤群等<sup>[35]</sup>由 Hamilton 原理建立轴向运动功能梯度 Timoshenko 梁运动微分方程组。邓昊等<sup>[36]</sup>求解了沿轴向指数分布的功能梯度 Timoshenko 梁的状态空间传递矩阵方程。随岁寒等<sup>[37]</sup>研究了轴向匀速运动功能梯度梁的稳定性,变速运动时的参数振动及其稳定性。

然而文献[9-20]只研究了轴向运动 Timoshenko 梁的振动特性,文献[34-35]也只研究了轴向运动功能梯度梁的振动特性,都未考虑磁场作用的影响;文献[21-28]只研究了磁场作用下轴向运动 Timoshenko 梁的振动特性,未涉及功能梯度材料的性质对振动特性的影响;文献[29-33,36]只研究了静态功能梯度梁的振动特性,未考虑陀螺项的影响。目前针对轴向运动结构的振动特性还存在一些问题,比如衰减系数和固有频率的对应性问题。本文研究了磁场中轴向运动功能梯度 Timoshenko 梁的振动特性,给出了其对应的控制方程组和简支边界条件。取适当参数,使用复模态法得到了速度和频率的对应关系,得到了前四阶固有频率和衰减系数,并通过微分求积法进行了验证。

## 1 控制方程

如图 1 所示,长  $l$ 、高  $h$ 、宽  $b$  的矩形梁,所受单位面积轴向拉力为  $P$ 。功能梯度导磁梁置于磁场强度为  $B(0, B_y, 0)$  的横向恒定磁场中,并以速度  $c$  沿  $x$  轴方向运动。

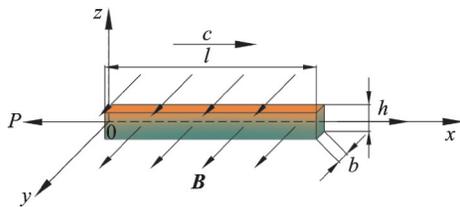


图 1 磁场作用下轴向运动功能梯度梁的物理模型

Fig. 1 The physical model of axially moving functionally graded beam under magnetic field

两种材料的弹性模量  $E(z)$ 、密度  $\rho(z)$ 、电导率  $\lambda(z)$ 、剪切模量  $G(z)$  均沿厚度方向按各组份体积以幂函数形式梯度变化

$$\Delta(z) = (\Delta_2 - \Delta_1) \left( \frac{z}{h} + \frac{1}{2} \right)^n + \Delta_1, \quad (1)$$

$$\Delta^T = (\lambda, E, G, \rho)$$

$$(\Delta A)_{\text{eq}} = \int_{-\frac{h}{2}}^{\frac{h}{2}} \int_{-\frac{b}{2}}^{\frac{b}{2}} \Delta(z) dy dz = h \left( \frac{1}{n+1} \Delta_2 + \frac{n}{n+1} \Delta_1 \right) \quad (2)$$

式中  $z$  为横截面上任意点距几何中面的距离,  $n$  为功能梯度指数,  $A = h \times b$  为截面积。

$$(EI)_{\text{eq}} = \int_{-\frac{h}{2}}^{\frac{h}{2}} \int_{-\frac{b}{2}}^{\frac{b}{2}} E(z) (z + z_0)^2 dy dz \quad (3)$$

$$(\rho I)_{\text{eq}} = \int_{-\frac{h}{2}}^{\frac{h}{2}} \int_{-\frac{b}{2}}^{\frac{b}{2}} \rho(z) (z + z_0)^2 dy dz \quad (4)$$

假设坐标原点建立在功能梯度材料梁的中性面上,功能梯度材料梁金属材料组分的体积比例系数  $V_n$  为梁厚度方向坐标  $z_1$  的幂函数

$$V_n = \left( \frac{z_1 - z_0}{h} + \frac{1}{2} \right)^n \quad (5)$$

式中  $n$  为梯度指数,  $z_0$  为梁中性面真实位置与文献[37]假设距梁上表面  $1/2$  处的中性面之间的距离。根据 Timoshenko 梁修正理论,假设  $\varphi$  为梁截面弯曲转角,可知功能梯度材料梁的正应力表达式为

$$\sigma = -E(z_1) z_1 \frac{\partial \varphi}{\partial x} \quad (6)$$

功能梯度梁弯曲时横截面正应力应满足以下表达式

$$\int_{z_0 - \frac{1}{2}h}^{z_0 + \frac{1}{2}h} \sigma dz_1 = \int_{z_0 - \frac{1}{2}h}^{z_0 + \frac{1}{2}h} -E(z_1) z_1 dz_1 = 0 \quad (7)$$

得到

$$z_0 = \frac{(E_2 - E_1)hn}{2(2+n)(E_2 + nE_1)} \quad (8)$$

轴向运动功能梯度梁受电磁场作用产生的感应电流密度

$$J_e = \lambda(\mathbf{V} \times \mathbf{B}) = \lambda \begin{vmatrix} \mathbf{i} & \mathbf{j} & \mathbf{k} \\ 0 & 0 & \frac{d\omega}{dt} \\ 0 & B_y & 0 \end{vmatrix} = -\lambda \frac{d\omega}{dt} B_y \mathbf{i} = -\lambda(\omega_{,t} + c\omega_{,x}) B_y \mathbf{i} \quad (9)$$

式中  $\omega(x, t)$  为梁运动时产生的横向振动位移,  $\mathbf{V}$  为速度矢量,  $\mathbf{i}$ ,  $\mathbf{j}$  和  $\mathbf{k}$  分别为沿坐标轴  $x$ ,  $y$  和  $z$  方向的单位向量。

感应电流密度产生的洛伦兹力为

$$\mathbf{f} = \mathbf{J} \times \mathbf{B} = \mathbf{J}_e \times \mathbf{B} = \begin{vmatrix} \mathbf{i} & \mathbf{j} & \mathbf{k} \\ J_e & 0 & 0 \\ 0 & B_y & 0 \end{vmatrix} = J_e B_y \mathbf{k} = -\lambda(\omega_{,t} + c\omega_{,x}) B_y^2 \mathbf{k} \quad (10)$$

动能为

$$T = \frac{1}{2} (\rho A)_{\text{eq}} \int_0^l (c + u_{,t} + cu_{,x})^2 dx + \frac{1}{2} (\rho A)_{\text{eq}} \int_0^l (\omega_{,t} + c\omega_{,x})^2 dx + \frac{1}{2} (\rho I)_{\text{eq}} \int_0^l (\varphi_{,t} + c\varphi_{,x})^2 dx \quad (11)$$

势能为

$$U = \int_0^l P(ds - dx) = \int_0^l P(\sqrt{1 + w_{,x}^2} - 1)dx \quad (12)$$

电磁虚功  $W_1$  的变化可写为

$$\delta W_1 = -A \int_0^l J_e B_y \delta w dx = (A\lambda)_{\text{eq}} \int_0^l B_y^2 (w_{,t} + cw_{,x}) \delta w dx \quad (13)$$

变形功  $W_2$  的变化可写为

$$\delta W_2 = - \int_{-\frac{h}{2}}^{\frac{h}{2}} \int_{-\frac{b}{2}}^{\frac{b}{2}} \int_0^l (\sigma_x \delta \epsilon_x + \tau_{zx} \delta \gamma_{zx}) dx dy dz \quad (14)$$

应力和应变分别为

$$\sigma_x = E(z) [\epsilon_x + \alpha(\epsilon_{x,t} + c\epsilon_{x,x})], \quad \epsilon_x = -(z + z_0) \varphi_{,x} + \sqrt{(1 + u_{,x})^2 + (w_{,x})^2} - 1 \quad (15)$$

$$\tau_{zx} = kG(z) [\gamma_{zx} + \alpha(\gamma_{zx,t} + c\gamma_{zx,x})], \quad \gamma_{zx} = w_{,x} - \varphi \quad (16)$$

式中  $\sigma_x(x, t)$  和  $\epsilon_x(x, t)$  分别为正应力和正应变,  $\tau_{zx}(x, t)$  和  $\gamma_{zx}(x, t)$  分别为剪应力和剪应变,  $k$  为 Timoshenko 梁的截面形状因子,  $\alpha$  为 Timoshenko 梁的黏弹性系数。

基于 Hamilton 原理

$$\delta \int_{t_1}^{t_2} (T - U) dt + \int_{t_1}^{t_2} \delta W dt = 0 \quad (17)$$

可以得到其无量纲形式的控制方程组和相应的简支边界条件:

$$w_{,tt} + 2\gamma w_{,xt} + (\eta\gamma^2 - 1)w_{,xx} + k_1(\varphi_{,x} - w_{,xx}) + \epsilon k_1 \alpha [\varphi_{,xt} - w_{,xxt} + \gamma(\varphi_{,xx} - w_{,xxx})] = -\beta(w_{,t} + \gamma w_{,x}) \quad (18)$$

$$k_2(\varphi_{,tt} + 2\gamma\varphi_{,xt} + \gamma^2\varphi_{,xx}) - k_f^2\varphi_{,xx} + k_1(\varphi - w_{,x}) = \epsilon\alpha \left\{ k_f^2(\varphi_{,xxt} + \gamma\varphi_{,xxx}) - k_1[\varphi_{,t} - w_{,xt} + \gamma(\varphi_{,x} - w_{,xx})] \right\} \quad (19)$$

$$w|_0^1 = 0, [(k_f^2 - k_2\gamma^2)\varphi_{,x} - k_2\gamma\varphi_{,t} + \epsilon k_f^2 \alpha (\varphi_{,xt} + \gamma\varphi_{,xx})]|_0^1 = 0 \quad (20)$$

式中  $\eta = 1/[1 + k_s/(2EA/l)]$  为支撑刚度参数;  $k_s$  为支撑刚度。支撑刚度参数的变化范围为 0-1。当支撑为完全刚性支撑时 ( $k_s \rightarrow +\infty$ ),  $\eta = 0$ ; 当支撑为完全柔性支撑时 ( $k_s = 0$ ),  $\eta = 1$ 。其他无量纲参数为

$$\begin{aligned} \sqrt{\epsilon} w &\leftrightarrow \frac{w}{l}, \sqrt{\epsilon} \varphi \leftrightarrow \varphi, x \leftrightarrow \frac{x}{l}, k_f = \sqrt{\frac{(EI)_{\text{eq}}}{P_0 l^2}}, \\ \eta &\leftrightarrow 1 - \eta, \epsilon\alpha \leftrightarrow \frac{\alpha}{l} \sqrt{\frac{P_0}{(\rho A)_{\text{eq}}}}, \gamma = c \sqrt{\frac{(\rho A)_{\text{eq}}}{P_0}}, \\ \beta &\leftrightarrow (A\lambda)_{\text{eq}} B_y^2 l \sqrt{\frac{1}{(\rho A)_{\text{eq}} P_0}}, k_1 = \frac{k(GA)_{\text{eq}}}{P_0}, \\ k_2 &= \frac{(\rho I)_{\text{eq}}}{(\rho A)_{\text{eq}} l^2}, t \leftrightarrow \frac{t}{l} \sqrt{\frac{P_0}{(\rho A)_{\text{eq}}}} \end{aligned} \quad (21)$$

## 2 复模态方法

假定式(18)和(19)具有分离变量的形式:

$$w(x, t) = \sum_{m=1}^{\infty} A_m(t) \phi_m(x) e^{\omega_m t} + cc \quad (22)$$

$$\varphi(x, t) = \sum_{m=1}^{\infty} B_m(t) \vartheta_m(x) e^{\omega_m t} + cc \quad (23)$$

式中  $cc$  表示前面各项的复共轭。四阶齐次线性复系数常微分方程组的解可以写为

$$\begin{cases} \phi_m = A_{1m} e^{\delta_{1m} x} + A_{2m} e^{\delta_{2m} x} + A_{3m} e^{\delta_{3m} x} + A_{4m} e^{\delta_{4m} x} \\ \vartheta_m = B_{1m} e^{\delta_{1m} x} + B_{2m} e^{\delta_{2m} x} + B_{3m} e^{\delta_{3m} x} + B_{4m} e^{\delta_{4m} x} \end{cases} \quad (24)$$

将式(22), (23)和(24)代入式(18)导出

$$B_m B_{jm} = C_{jm} A_m A_{jm} \quad (25)$$

其中

$$C_{jm} = -[\omega_m(\omega_m + \beta) + \gamma(2\omega_m + \beta)\delta_{jm} + (-1 + \eta\gamma^2 - k_1)\delta_{jm}^2] / (k_1 \delta_{jm}) \quad (26)$$

解耦式(18)和(19), 并将式(22), (23)和(24)

代入解耦后的式子得到

$$\begin{aligned} &(\gamma^2 k_2 - k_f^2) \left( \frac{\gamma^2 \eta - 1}{k_1} - 1 \right) \delta_{jm}^4 + \\ &\left\{ -2\omega_m \gamma^2 \left[ \frac{k_2(5\gamma^2 + \gamma^2 \eta - 1) - k_f^2}{k_1} - k_2 \right] + \frac{\beta\gamma(k_f^2 - \gamma^2 k_2)}{k_1} \right\} \delta_{jm}^3 - \\ &\left\{ \omega_m^2 \left[ \frac{k_2(5\gamma^2 + \eta\gamma^2 - 1) - k_f^2}{k_1} - k_2 \right] - \omega_m \frac{\beta(k_f^2 - 3\gamma^2 k_2)}{k_1} + \gamma^2 \eta - 1 \right\} \delta_{jm}^2 - \\ &\left( \omega_m^3 \frac{4\gamma k_2}{k_1} + \omega_m^2 \frac{3\beta\gamma k_2}{k_1} + 2\omega_m \gamma + \beta\gamma \right) \delta_{jm} - \\ &\left( \omega_m^4 \frac{k_2}{k_1} + \omega_m^3 \frac{\beta k_2}{k_1} + \omega_m^2 + \omega_m \beta \right) = 0 \end{aligned} \quad (27)$$

整理得到频率方程

$$\begin{aligned} & \left[ e^{(\delta_{1m} + \delta_{2m})} + e^{(\delta_{3m} + \delta_{4m})} \right] (D_{1m} - D_{2m})(D_{3m} - D_{4m}) - \\ & \left[ e^{(\delta_{1m} + \delta_{3m})} + e^{(\delta_{2m} + \delta_{4m})} \right] (D_{1m} - D_{3m})(D_{2m} - D_{4m}) + \\ & \left[ e^{(\delta_{2m} + \delta_{3m})} + e^{(\delta_{1m} + \delta_{4m})} \right] (D_{2m} - D_{3m})(D_{1m} - D_{4m}) = 0 \quad (28) \end{aligned}$$

从而导出模态函数

$$\begin{aligned} \phi_m = a_1 & \left\{ e^{\delta_{1m}x} - \frac{(D_{4m} - D_{1m})(e^{\delta_{3m}} - e^{\delta_{1m}})}{(D_{4m} - D_{2m})(e^{\delta_{3m}} - e^{\delta_{2m}})} e^{\delta_{2m}x} - \right. \\ & \frac{(D_{4m} - D_{1m})(e^{\delta_{2m}} - e^{\delta_{1m}})}{(D_{4m} - D_{3m})(e^{\delta_{2m}} - e^{\delta_{3m}})} e^{\delta_{3m}x} - \\ & \left[ 1 - \frac{(D_{4m} - D_{1m})(e^{\delta_{3m}} - e^{\delta_{1m}})}{(D_{4m} - D_{2m})(e^{\delta_{3m}} - e^{\delta_{2m}})} - \right. \\ & \left. \frac{(D_{4m} - D_{1m})(e^{\delta_{2m}} - e^{\delta_{1m}})}{(D_{4m} - D_{3m})(e^{\delta_{2m}} - e^{\delta_{3m}})} \right] e^{\delta_{4m}x} \left. \right\} \quad (29) \end{aligned}$$

$$\begin{aligned} \vartheta_m = a_1 & \left\{ -\frac{C_{2m}(D_{4m} - D_{1m})(e^{\delta_{3m}} - e^{\delta_{1m}})}{(D_{4m} - D_{2m})(e^{\delta_{3m}} - e^{\delta_{2m}})} e^{\delta_{2m}x} + \right. \\ & C_{1m} e^{\delta_{1m}x} - \frac{C_{3m}(D_{4m} - D_{1m})(e^{\delta_{2m}} - e^{\delta_{1m}})}{(D_{4m} - D_{3m})(e^{\delta_{2m}} - e^{\delta_{3m}})} e^{\delta_{3m}x} - \\ & \left. C_{4m} \left[ 1 - \frac{(D_{4m} - D_{1m})(e^{\delta_{3m}} - e^{\delta_{1m}})}{(D_{4m} - D_{2m})(e^{\delta_{3m}} - e^{\delta_{2m}})} - \right. \right. \\ & \left. \left. \frac{(D_{4m} - D_{1m})(e^{\delta_{2m}} - e^{\delta_{1m}})}{(D_{4m} - D_{3m})(e^{\delta_{2m}} - e^{\delta_{3m}})} \right] e^{\delta_{4m}x} \right\} \quad (30) \end{aligned}$$

其中

$$\begin{aligned} D_{jm} = & -[\omega_m^2 + \beta\omega_m + \gamma(2\omega_m + \beta)]\delta_{jm} - \\ & (1 - \gamma^2\eta + k_1)\delta_{jm}^2 \left[ -k_f^2\delta_{jm} + \gamma k_2(\omega_m + \gamma\delta_{jm}) \right] / \delta_{jm}, \\ & j = 1, 2, 3, 4 \quad (31) \end{aligned}$$

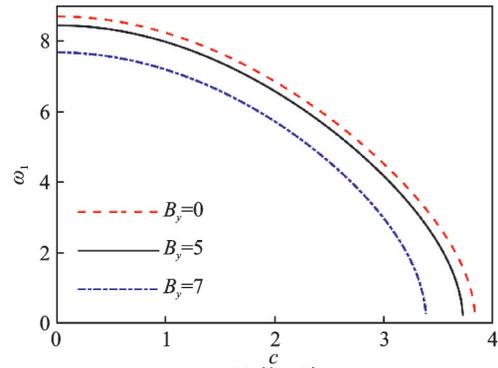
给定陶瓷和金属材料的物性参数如表1所示,若给定  $n=1, \lambda=1.17 \times 10^6, \eta=0.5, k_1=76.1836, k_2=4.4 \times 10^{-3}, k_f=0.8781$  和  $\gamma=2$ , 对于不同的磁场强度  $B_y$ , 前两阶固有频率随轴向速度的变化如图2所示。当  $B_y=2.5, n=1$  时, 在不同支撑刚度参数下前两阶固有频率随轴向速度的变化如图3所示。当  $B_y=2.5, \eta=0.5$  时, 在不同功能梯度指数下前两阶固有频率随轴向速度的变化如图4所示。

从图2-4中可以明显看出, 固有频率随着轴速

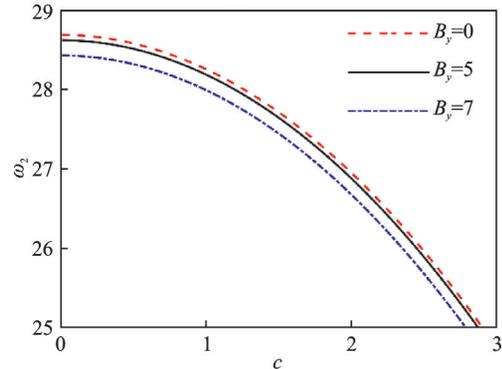
表1 陶瓷和金属材料的物性参数

Tab. 1 Physical properties of ceramic and metal materials

材料	弹性模量/GPa	泊松比 $\mu$	密度/( $\text{kg} \cdot \text{m}^{-3}$ )	电导率/( $\Omega \cdot \text{m}$ )
金属 Ti-6Al-4V	122.56	0.3	3000	$2.34 \times 10^6$
陶瓷 Zirconia	244.27	0.3	4429	0

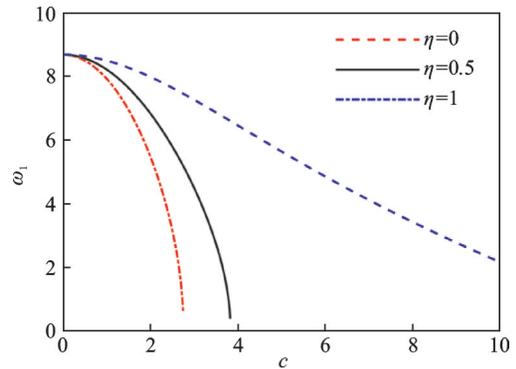


(a) 第一阶  
(a) First order

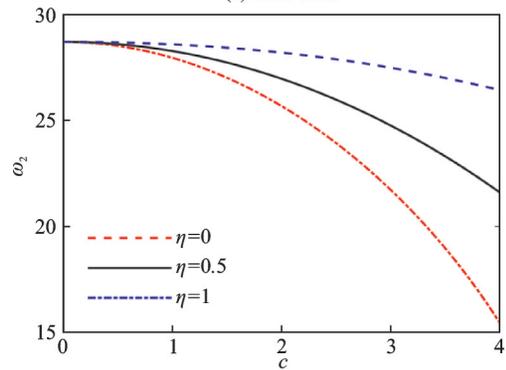


(b) 第二阶  
(b) Second order

图2 不同磁场强度下前两阶固有频率随轴向速度的变化  
Fig. 2 The variation of the first two natural frequencies with axial velocity under different magnetic field intensities



(a) 第一阶  
(a) First order



(b) 第二阶  
(b) Second order

图3 不同支撑刚度参数下前两阶固有频率随轴向速度的变化  
Fig. 3 The variation of the first two natural frequencies with axial velocity under different support stiffness parameters

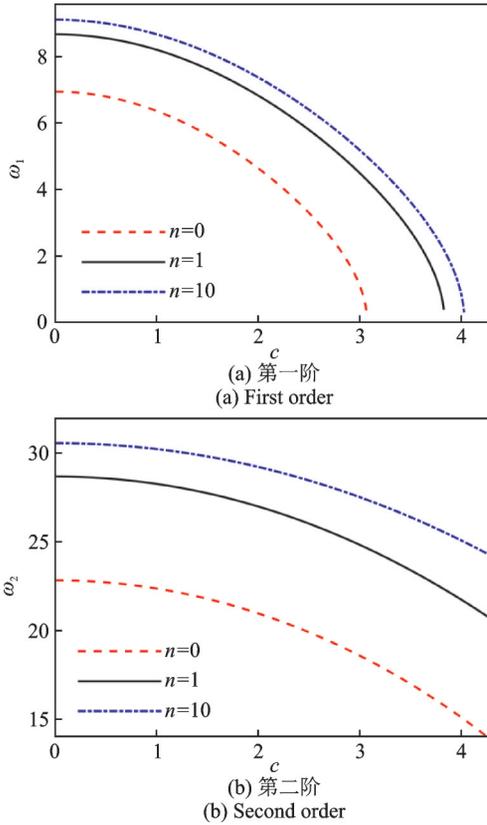


图4 不同功能梯度指数下前两阶固有频率随轴向速度的变化  
Fig. 4 The variation of the first two natural frequencies with axial velocity under different functional gradient indices

的增加而连续减小。当固定轴向运动速度时,从图2(a)中可以看出,较大的磁场强度对应较小的固有频率;从图2(b)中可以看出,磁场强度对于二阶固有频率的影响较小。因此,磁场强度的引入,使一阶系统的临界速度有了明显的减小。从图3中可以看出,当固定轴向运动速度时,较大的支撑刚度参数对应较大的固有频率。因此,支撑刚度参数的引入,使系统的临界速度有了显著的增加。当固定轴速时,从图4中可以看出,较大的功能梯度指数对应较小的固有频率。功能梯度梁的固有频率在两种材料非功能梯度梁的固有频率之间随 $n$ 的变化而变化。

### 3 数值验证

本节引入微分求积法<sup>[38-40]</sup>对以上近似解析解进行数值验证。Timoshenko梁的计算区域为 $x \in [0, 1]$ 。 $x$ 方向的网点数为 $N$ 。通过微分求积法将控制方程(18)-(20)离散为:

$$\begin{aligned} & \omega_m^2 \phi_m + 2\gamma \omega_m \sum_{k=2}^{N-1} A_{mk}^{(1)} \phi_k + (\eta\gamma^2 - k_1 - 1) \sum_{k=2}^{N-1} A_{mk}^{(2)} \phi_k + \\ & k_1 \sum_{k=1}^N A_{mk}^{(1)} \vartheta_k + \beta \omega_m \phi_m + \beta \gamma \sum_{k=1}^N A_{mk}^{(1)} \phi_k = 0, \\ & m = 2, 3, \dots, N-1 \end{aligned} \quad (32)$$

$$k_2 \left( \omega_m^2 \vartheta_i + 2\omega_m \gamma \sum_{k=1}^N A_{mk}^{(1)} \vartheta_k \right) + (k_2 \gamma^2 - k_i^2) \sum_{k=1}^N A_{mk}^{(2)} \vartheta_k + k_1 \left( \vartheta_m - \sum_{k=1}^{N-1} A_{mk}^{(1)} \vartheta_k \right) = 0, m = 2, 3, \dots, N-1 \quad (33)$$

$$\begin{aligned} & (k_i^2 - k_2 \gamma^2) \sum_{k=1}^N A_{mk}^{(1)} \vartheta_k - \omega_m k_2 \gamma \vartheta_m = 0, \\ & m = 1, N \end{aligned} \quad (34)$$

应用修正权系数法修正后写为矩阵形式

$$(\omega_m^2 \mathbf{M} + \omega_m \mathbf{G} + \mathbf{K}) \mathbf{S} = 0 \quad (35)$$

式中  $\mathbf{M}$ ,  $\mathbf{G}$  和  $\mathbf{K}$  分别为质量矩阵、陀螺矩阵和刚度矩阵。它们的维数均为  $2N \times 2N$ 。 $\mathbf{S}$  表征广义矩阵,其维数为  $2N \times 1$ 。

给定  $N=15$ ,  $n=1$ ,  $B_y=2.5$ ,  $\lambda=1.17 \times 10^6$ ,  $\eta=0.5$ ,  $k_1=76.1836$ ,  $k_2=4.4 \times 10^{-3}$ ,  $k_i=0.8781$  和  $\gamma=2$ , 图5给出了线性派生系统前四阶的衰减系数和固有频率随着轴向速度的变化情况的两种处理结果的比较。 $\delta_1, \delta_2, \delta_3, \delta_4$  分别表示前四阶的衰减系数;  $\omega_1, \omega_2, \omega_3, \omega_4$  分别表示前四阶相应的固有频率。从中可以看出,衰减系数呈现不对称性。图6为图5中点a, b, c位置放大图。图中连续的线表示解析出的前四阶衰减率以及固有频率,不连续的点则表示数值分析的结果。对比结果表明,解析的结果与数值分析的结果在数值上是十分相近的。当不考虑磁场时,一阶与二阶、一阶与三阶、二阶与四阶固有频率分别在点a, b, c处产生耦合,三点处相关的固有频率完

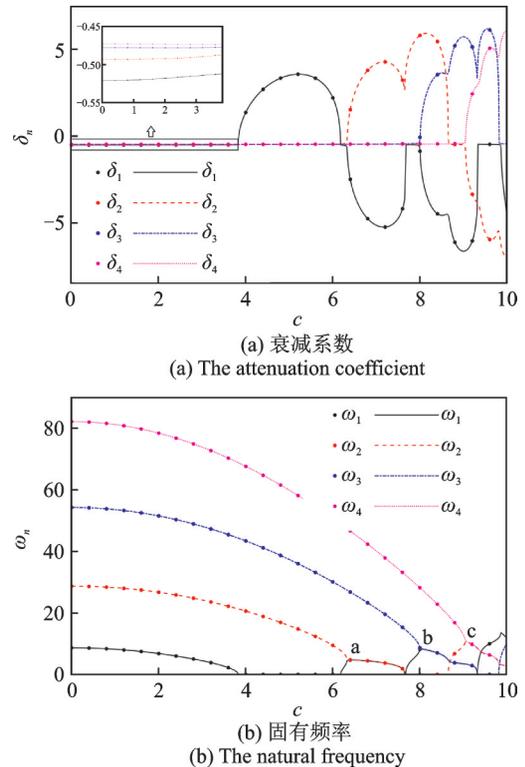


图5 前四阶衰减系数和固有频率随轴向速度的变化  
Fig. 5 The attenuation coefficients and the natural frequencies of the first four orders vary with axial velocity

全相等(相应的衰减系数不同),不会出现分离。当考虑磁场时,三点处相关的固有频率依然存在耦合,但是数值已有差别,此时耦合固有频率具有分离特性。

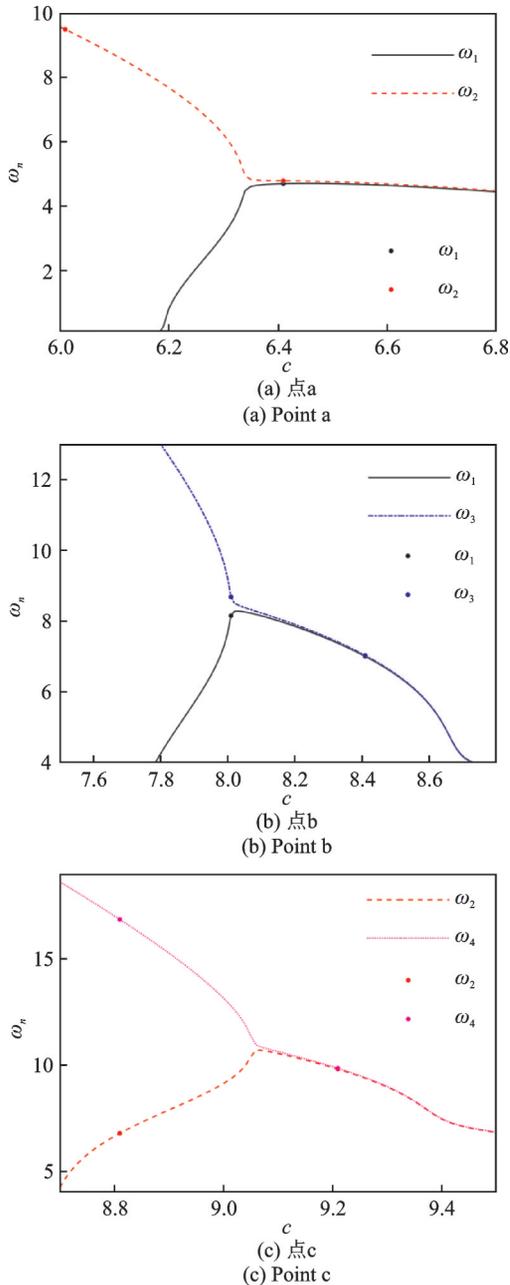


图 6 点 a, b, c 放大图

Fig. 6 Partial magnifications of points a, b and c

## 4 结 论

本文运用复模态法和微分求积法研究了磁场作用下轴向运动功能梯度 Timoshenko 梁的振动特性。通过一系列的数值算例,描述了磁场强度、功能梯度指数和支撑刚度参数变化对固有频率的影响。研究结果表明:随着轴向运动速度的增大,梁的固有频率减小的速度越来越快。随着磁场强度和功能梯度指

数的增大,梁的固有频率减小;随着支撑刚度参数的增大,梁的固有频率增大,但其随轴向速度的增大而减小的速度越来越慢。磁场强度的变化对于第二阶固有频率影响并不明显。衰减系数呈现不对称性,耦合固有频率呈现分离性。

## 参考文献:

- [1] Aiken J. An account of some experiments on rigidity produced by centrifugal force [J]. The London, Edinburgh, and Dublin Philosophical Magazine and Journal of Science, 1878, 5(29): 81-105.
- [2] Mote C D Jr. Dynamic stability of axially moving materials[J]. The Shock and Vibration Digest, 1972, 4(4): 2-11.
- [3] Wickert J A, Mote C D Jr. Current research on the vibration and stability of axially-moving materials[J]. The Shock and Vibration Digest, 1988, 20(5):3-13.
- [4] Wang K W, Liu S P. On the noise and vibration of chain drive system [J]. The Shock and Vibration Digest, 1991, 23(4): 8-13.
- [5] Pellicano F, Vestroni F. Nonlinear dynamics and bifurcations of an axially moving beam[J]. Journal of Vibration and Acoustics, 2000, 122(1): 21-30.
- [6] Ouyang H J. Moving-load dynamic problems: A tutorial (with a brief overview)[J]. Mechanical Systems and Signal Processing, 2011, 25(6): 2039-2060.
- [7] Malookani R A, Van Horssen W T. On resonances and the applicability of Galerkin's truncation method for an axially moving string with time-varying velocity [J]. Journal of Sound and Vibration, 2015, 344: 1-17.
- [8] 陈立群. 轴向运动结构的能量关系和守恒量研究进展 [J]. 北京大学学报(自然科学版), 2016, 52(4): 727-731.  
Chen Liqun. Research progress on energy relations and conserved quantities of axial motion structures[J]. Acta Scientiarum Naturalium Universitatis Pekinensis, 2016, 52(4): 727-731.
- [9] 王 乐, 余慕春. 轴力对自由边界 Timoshenko 梁横向动特性影响研究 [J]. 兵器装备工程学报, 2018, 39(3):36-39.  
Wang Le, Yu Muchun. Research on the influence of axial force on the lateral dynamic characteristics of free boundary Timoshenko beam [J]. Journal of Ordnance Equipment Engineering, 2018, 39(3):36-39.
- [10] Tang Y Q, Chen L Q, Yang X D. Natural frequencies, modes and critical speeds of axially moving Timoshenko beams with different boundary conditions [J]. International Journal of Mechanical Sciences, 2008, 50(10-11): 1448-1458.
- [11] 杨晓东, 唐有琦, 戈新生. 轴向运动 Timoshenko 梁固

- 有频率的求解方法研究[J]. 机械强度, 2009, 31(2): 208-210.
- Yang Xiaodong, Tang Youqi, Ge Xinsheng. Research on the method of solving the natural frequency of the axially moving Timoshenko beam[J]. Journal of Mechanical Strength, 2009, 31(2): 208-210.
- [12] 刘星光, 唐有绮, 周 远. 三种典型轴向运动结构的振动特性对比[J]. 力学学报, 2020, 52(2): 522-532.
- Liu Xingguang, Tang Youqi, Zhou Yuan. Comparison of vibration characteristics of three typical axially moving structures[J]. Theoretical and Applied Mechanics, 2020, 52(2): 522-532.
- [13] Ghayesh M H, Balar S. Non-linear parametric vibration and stability analysis for two dynamic models of axially moving Timoshenko beams [J]. Applied Mathematical Modelling, 2010, 34(10): 2850-2859.
- [14] Chen L Q, Tang Y Q, Lim C W. Dynamic stability in parametric resonance of axially accelerating viscoelastic Timoshenko beams [J]. Journal of Sound and Vibration, 2010, 329(5): 547-565.
- [15] Ghayesh M H, Amabili M. Nonlinear vibrations and stability of an axially moving Timoshenko beam with an intermediate spring support [J]. Mechanism and Machine Theory, 2013, 67: 1-16.
- [16] 周 远, 唐有绮, 刘星光. 黏弹性阻尼作用下轴向运动 Timoshenko 梁振动特性的研究 [J]. 力学学报, 2019, 51(6): 1897-1904.
- Zhou Yuan, Tang Youqi, Liu Xingguang. Study on vibration characteristics of axially moving Timoshenko beam under viscoelastic damping [J]. Theoretical and Applied Mechanics, 2019, 51(6): 1897-1904.
- [17] 唐有绮. 轴向变速黏弹性 Timoshenko 梁的非线性振动 [J]. 力学学报, 2013, 45(6): 965-973.
- Tang Youqi. Nonlinear vibration of viscoelastic Timoshenko beam with axially variable speed [J]. Theoretical and Applied Mechanics, 2013, 45(6): 965-973.
- [18] An C, Su J. Dynamic response of axially moving Timoshenko beams; Integral transform solution [J]. Applied Mathematics and Mechanics, 2014, 35(11): 1421-1436.
- [19] Tang Y Q, Chen L Q, Yang X D. Parametric resonance of axially moving Timoshenko beams with time-dependent speed [J]. Nonlinear Dynamics, 2009, 58(4): 715-724.
- [20] Chen L Q, Tang Y Q, Lim C W. Dynamic stability in parametric resonance of axially accelerating viscoelastic timoshenko beams [J]. Journal of Sound and Vibration, 2010, 329(5): 547-565.
- [21] HU Yu-da, ZHANG Li-bao. Magneto-elastic vibration equations for axially moving conductive and magnetic beams [J]. Applied Mathematics & Mechanics, 2015, 36(1): 70-77.
- [22] 张立保, 胡宇达. 磁场中轴向运动导电梁弯曲自由振动分析 [J]. 力学季刊, 2015, 36(1): 141-147.
- Zhang Libao, Hu Yuda. Analysis of bending free vibration of an axially moving conductive beam in a magnetic field [J]. Chinese Quarterly of Mechanics, 2015, 36(1): 141-147.
- [23] 郑晓静, 刘信恩. 铁磁导电梁式板在横向均匀磁场中的动力特性分析 [J]. 固体力学学报, 2004, 21(3): 243-250.
- Zheng Xiaojing, Liu Xinen. Analysis of dynamic characteristics of ferromagnetic conductive beam plate in transverse uniform magnetic field [J]. Chinese Journal of Solid Mechanics, 2004, 21(3): 243-250.
- [24] 周又和, 郑晓静. 电磁固体结构力学 [M]. 北京: 科学出版社, 1999.
- Zhou Youhe, Zheng Xiaojing. Electromagnetic Solid Structure Mechanics [M]. Beijing: Science Press, 1999.
- [25] 王 杰, 胡宇达. 磁场中轴向运动载流梁磁弹性主共振分析 [J]. 振动与冲击, 2016, 35(23): 65-72.
- Wang Jie, Hu Yuda. Analysis of the main magnetoelastic resonance of an axially moving current-carrying beam in a magnetic field [J]. Journal of Vibration and Shock, 2016, 35(23): 65-72.
- [26] 胡宇达, 张明冉. 两平行导线间轴向运动载流梁的非线性主共振 [J]. 工程力学, 2018, 35(10): 238-248.
- Hu Yuda, Zhang Mingran. Nonlinear primary resonance of an axially moving current-carrying beam between two parallel wires [J]. Engineering Mechanics, 2018, 35(10): 238-248.
- [27] Liu Hui-feng, Li Jun-lin, Yang Dong-hui. Displacement response of nonlinear free vibration of an axially moving current-conducting beam in magnetic field [J]. Journal of Southwest Minzu University (Natural Science Edition), 2017, 43(04): 418-423.
- [28] 崔 雪. 磁场中轴向运动铁磁梁的固有振动 [D]. 秦皇岛: 燕山大学, 2019.
- Cui Xue. Natural vibration of an axially moving ferromagnetic beam in a magnetic field [D]. Qinhuangdao: Yanshan University, 2019.
- [29] Su H, Banerjee J R. Development of dynamic stiffness method for free vibration of functionally graded Timoshenko beams [J]. Computers & Structures, 2015, 147: 107-116.
- [30] Zhong Z, Yu T. Analytical solution of a cantilever functionally graded beam [J]. Composites Science & Technology, 2007, 67(3-4): 481-488.
- [31] Alshorbagy A E, Eltahir M A, Mahmoud F F. Free vibration characteristics of a functionally graded beam by finite element method [J]. Applied Mathematical Modelling, 2011, 35(1): 412-425.

- [32] Lai S K, Harrington J, Xiang Y, et al. Accurate analytical perturbation approach for large amplitude vibration of functionally graded beams [J]. *International Journal of Non-Linear Mechanics*, 2012, 47(5): 473-480.
- [33] Thai H T, Vo T P. Bending and free vibration of functionally graded beams using various higher-order shear deformation beam theories [J]. *International Journal of Mechanical Sciences*, 2012, 62(1): 57-66.
- [34] 刘金建, 蔡改改, 谢 锋. 轴向运动功能梯度粘弹性梁横向振动的稳定性分析 [J]. *动力学与控制学报*, 2016, (6): 533-541.  
Liu Jinjian, Cai Gaigai, Xie Feng. Stability analysis of lateral vibration of functionally graded viscoelastic beam with axial motion [J]. *Journal of Dynamics and Control*, 2016, (6): 533-541.
- [35] 赵凤群, 王忠民, 路小平. 轴向运动功能梯度 Timoshenko 梁稳定性分析 [J]. *振动与冲击*, 2014, 33(2): 14-19.  
Zhao Fengqun, Wang Zhongmin, Lu Xiaoping. Stability analysis of functionally graded Timoshenko beam with axial motion [J]. *Journal of Vibration and Shock*, 2014, 33(2): 14-19.
- [36] 邓 昊, 程 伟. 沿轴向指数分布的功能梯度 Timoshenko 梁的频率精确解 [J]. *振动与冲击*, 2017, 36(6): 91-96.  
Deng Hao, Cheng Wei. Accurate frequency solution of functionally graded Timoshenko beam with exponential distribution along the axial direction [J]. *Journal of Vibration and Shock*, 2017, 36(6): 91-96.
- [37] 随岁寒. 轴向运动功能梯度梁的动力学分析 [D]. 苏州: 苏州大学, 2015.
- [38] Chen Hongyong, Li Shangming. Study on dynamic characteristics of axial moving beam under axial load [J]. *Journal of Vibration and Shock*, 2016, 35(19): 75-80.
- [39] Ding Hu. Numerical investigation into nonlinear parametric resonance of axially moving accelerating viscoelastic beams [J]. *Chinese Journal of Computational Mechanics*, 2012, 29(4): 545-550.
- [40] Bert C W, Malik M. The differential quadrature method in computational mechanics: A review [J]. *Applied Mechanics Reviews*, 1996, 49: 1-28.

## The vibration characteristics of axially moving functionally graded Timoshenko beam under magnetic field

CHEN Xi, TANG You-qi, LIU Shuang

(School of Mechanical Engineering, Shanghai Institute of Technology, Shanghai 201418, China)

**Abstract:** Engineering vibration of the axially moving structure always has been one of the important topics in the field of dynamics. In order to analyze the vibration in the project more completely, this paper discusses in detail the vibration characteristics of the axially moving functionally graded Timoshenko beam under magnetic field. The dynamic equations and corresponding simply supported boundary conditions of the axially moving functionally graded Timoshenko beam under the magnetic field are obtained. The complex modal method is used to obtain the corresponding relation between the natural frequencies and the attenuation coefficients and the axial speeds with different parameters. The differential quadrature method is used to analyze the variation of the first four order natural frequencies and attenuation coefficients with axial speed under the magnetic field. The results are compared with those of the complex mode method. The results show that the solution obtained by the complex modal method is an exact analytical solution. The attenuation coefficient is asymmetrical and the coupling natural frequency is separable. As the axial speed, the magnetic field strength, and functional gradient index increase, the natural frequency decreases. The natural frequency increases with the increase of the support stiffness parameter.

**Key words:** Timoshenko beam; functionally graded materials; complex modal method; natural frequency; attenuation coefficient

作者简介: 陈 喜(1995-), 男。电话: 15890005093; E-mail: 593207810@qq.com

通讯作者: 柳 爽(1986-), 女, 副教授。电话: (021)60873024; E-mail: lsbbsh@126.com